

Ice in the 1994 Rabaul eruption cloud: implications for volcano hazard and atmospheric effects

W. I. Rose*, D. J. Delene*, D. J. Schneider*,
G. J. S. Bluth*, A. J. Krueger†, I. Sprod†,
C. McKee‡, H. L. Davies§ & G. G. J. Ernst||

* Geological Engineering and Sciences,
Michigan Technological University, Houghton, Michigan 49931, USA

† NASA Goddard Space Flight Center, Greenbelt, Maryland 20771,
USA

‡ Rabaul Volcano Observatory, PO Box 386, Rabaul,
Papua New Guinea

§ University of Papua New Guinea, PO Box 414, University,
Papua New Guinea

|| Department of Geology, University of Bristol, Bristol BS8 1RJ, UK

VOLCANIC clouds are an important natural hazard to aircraft¹, and host chemical reactions that interest both volcanologists^{2,3} and atmospheric scientists⁴⁻⁶. Ice has been suggested as a possible component of eruption clouds⁷, but there has been no direct evidence for its presence. Here we report the detection, using a satellite-borne infrared sensor, of ≥ 2 million tonnes of ice in the cloud produced by the September 1994 eruption of Rabaul volcano, in Papua New Guinea. The cloud also contained relatively low levels of sulphur dioxide (80 ± 50 kilotonnes), compared with other stratospheric eruption clouds. The unusual aspects of this cloud may be related to the entry of sea water into the volcanic vent, and its participation in the eruption column. Past eruptions that occurred in similar (coastal) settings, such as those of Krakatau and Santorini, might have had less effect on the atmosphere than their volume alone would suggest, because the presence of ice may decrease the residence time of ash and sulphur in the atmosphere. In addition, the ability of ice to mask the characteristic spectral signature of volcanic ash will increase the difficulty of designing airborne ash detection systems for aviation safety.

The 1994 Rabaul eruption began on 19 September with nearly simultaneous outbursts from two vents (Tavurvur, 06:06 local time; Vulcan, 07:17 local time) on opposite sides of the caldera (Fig. 1 inset). The Vulcan eruption was more powerful, with column heights estimated at 20 km, whereas Tavurvur's column reached a maximum height⁸ of 6 km. Some of the ash fallout was very wet, and a 'rain of mud' occurred in some areas around Rabaul. Sea water had access to the main active vent low on the northeastern flank of Vulcan, and salty rainfalls took place in a wide arc north and northwest of Vulcan during 19 and 20 September⁸. The tephra fall deposits resulting from Vulcan's eruptions contained ubiquitous sea-salt deposits.

The advanced very-high-resolution radiometer (AVHRR) detector aboard the NOAA 12 polar-orbiting satellite was used for mapping the volcanic cloud and determining the composition, size and mass of its particles based on data collected on 19 September at 09:00 UT (19:00 local time) and again at 21:50 UT (20 September, 07:50 local time). The dispersal pattern shown by the Rabaul cloud was marked by a broad fan shape (Fig. 2),

probably caused in part by upper-level winds; many volcanic clouds, particularly at middle and high latitudes, are more directionally focused⁹ than this.

Multi-wavelength AVHRR images have two thermal infrared channels (band 4, $\lambda = 10.3-11.3 \mu\text{m}$; band 5, $\lambda = 11.5-12.5 \mu\text{m}$) which can be used for estimation of the sizes, masses and some compositional characteristics of particles in the cloud¹⁰. Silicate ash and concentrated sulphuric acid aerosol particles in transparent drifting volcanic clouds have distinctive negative band 4-band 5 apparent temperature differences¹¹⁻¹⁴. Figure 3a shows a plot of band 4-band 5 temperature differences versus band 4 temperatures for the individual pixels comprising Fig. 2. For comparison, Fig. 3b shows a similar plot for the volcanic cloud arising from the Klyuchevskoi eruption. The Klyuchevskoi cloud is representative of many volcanic clouds which have negative band 4-band 5 temperature differences. The positive band 4-5 temperature difference exhibited by the Rabaul cloud is unique among a dozen eruptions that we have studied with this method¹³; the volcanic cloud shows no silicate or sulphate signal. The observed temperature differences were compared with simulated temperature differences calculated using refractive indices for ice (Fig. 3a), which demonstrates that Rabaul's cloud had the spectral characteristics of spherical ice particles with effective radii of 9-40 μm . (In reality, the cloud will have contained particles with radii outside this range.) Note that the temperature of the opaque portion of the Rabaul eruption cloud is $\sim 190 \text{ K}$ (-83°C), corresponding to the inferred tropopause temperature from the radiosonde data.

We compare Rabaul to the Klyuchevskoi eruption because the Klyuchevskoi cloud is much more like other volcanic clouds we have studied, was similar in scale to Rabaul, although smaller, and was examined by the same AVHRR detector only 12 days after it observed Rabaul's cloud. The Klyuchevskoi cloud contained more SO_2 than Rabaul's, although little ice, and was driven by stronger ($40-65 \text{ m s}^{-1}$) northwesterly winds at an altitude of 12-13 km. The Klyuchevskoi cloud exhibited no significant wind shear (P. Newman, personal communication) and a focused dispersal pattern which extended in an elongated plume across the northern Pacific. The effective radii of the ice particles in the Rabaul cloud are larger than the particle sizes that we have observed in volcanic clouds with silicate signals, such as Klyuchevskoi. The effective particle radius inferred for the Klyuchevskoi eruption cloud was in the range 1-12 μm .

Using the methods of Wen and Rose¹⁰, we computed the total masses of ice in the transparent (optical depth < 4) parts of the Rabaul cloud and found a mass of 2-3 megatonnes (Mt). This mass is ten times the mass of silicates calculated for the Klyuchevskoi cloud (0.1-0.3 Mt). The particle mass contained in the transparent part of a volcanic cloud during an eruption is a small fraction ($< 1\%$) of the total¹⁰, as most of the mass is in the opaque near-vent portion of the cloud. The opaque por-

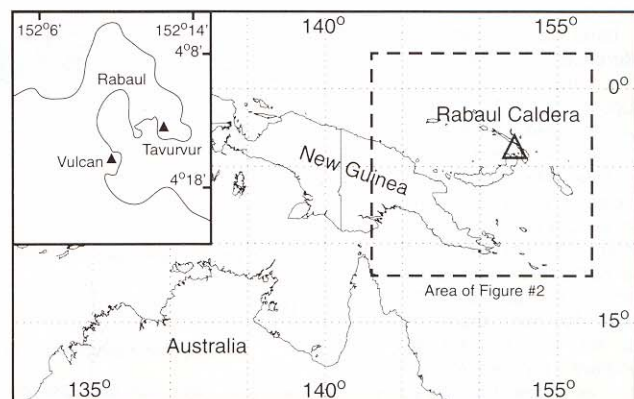


FIG. 1 Location maps for Rabaul caldera.

tion of Rabaul's cloud (optical depth >4) makes up <5% of the total area (Fig. 2) but must contain all of the large particles (>1 mm in diameter), which fall out in less than 30 minutes before they travel more than a few tens of kilometres. Smaller particles fall out more slowly but represent a small fraction of the total particle mass in the cloud. For instance, a 13-hour-old drifting cloud from the September 1992 Spurr eruption contained a mass equivalent to <1% of the mass that fell out in the ash-fall blanket¹⁰. We cannot measure the masses in the dense opaque portion of Rabaul's cloud near the vent, where fallout is highly concentrated and particles are largest, but based on analogy with the Spurr cloud, we conclude that the total ice mass in the Rabaul cloud is likely to be at least 100 times higher than our estimate for the transparent cloud.

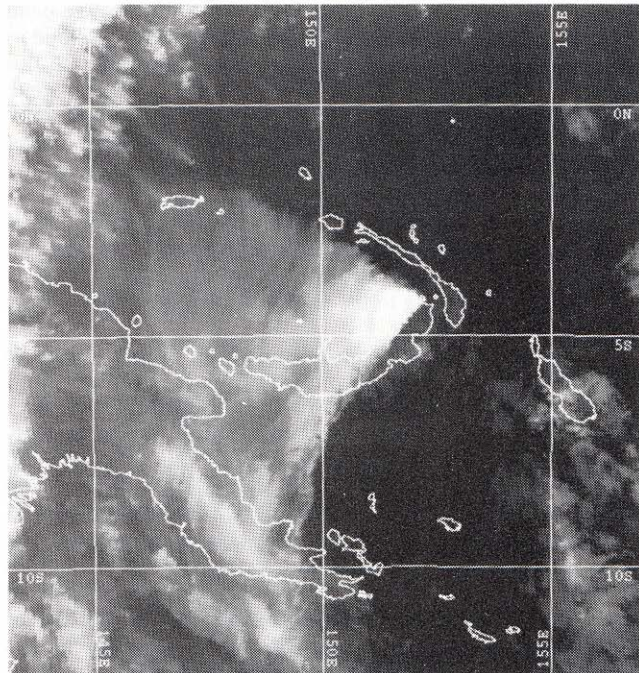
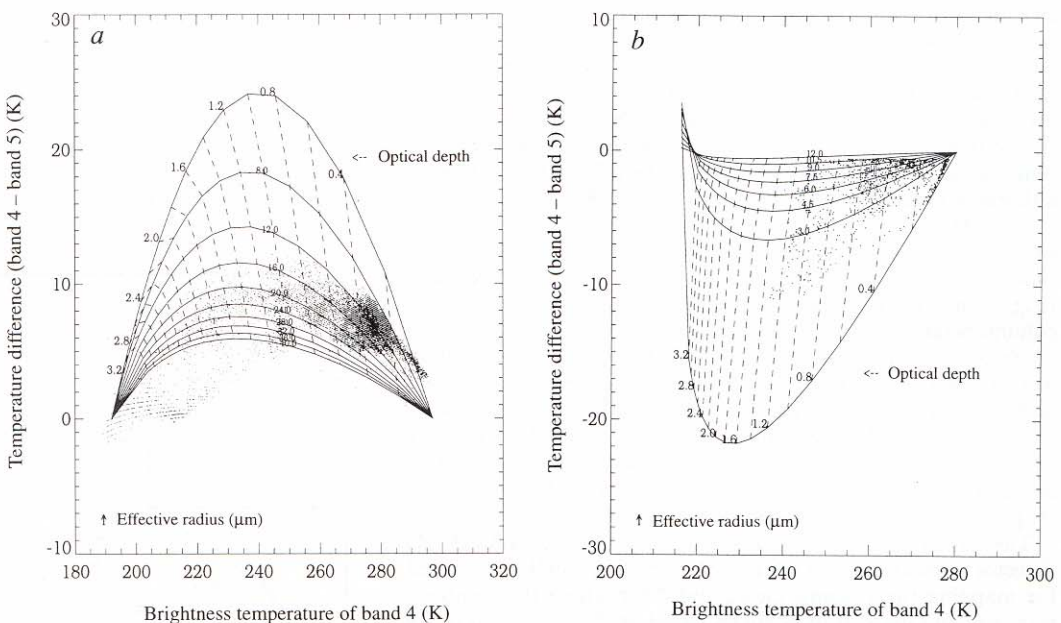


FIG. 2 AVHRR image of the Rabaul eruption cloud at 09:00 UT, 19 September 1994, showing band 4 data with the coldest temperatures shown by the brightest pixels. The temperature of the opaque part of the Rabaul cloud (optical depth >4) is ~190 K. Most of the cloud is transparent, and the warmer surface below transmits through the cold cloud, resulting in higher measured temperatures. The transparent part of this cloud is used for the plot of individual pixel values in Fig. 3a. High-level winds and temperature profiles were obtained through NASA's Goddard Space Flight Center from several radiosonde stations surrounding Rabaul for 18 and 19 September at 23:00 UT each day (the closest being the station at Momote, ~540 km WNW of Rabaul). They show the tropopause at an altitude of 16 km, with a temperature of 190 K. The prevailing winds exhibit wind shear, with generally stronger (initially 25–35 and increasing to 50–60 m s⁻¹) northeasterly winds at 10–13 km height and weaker (15–45 m s⁻¹) ESE winds at 16–21 km (P. Newman, personal communication).

FIG. 3 Band 4 – band 5 temperature differences plotted versus band 4 brightness temperatures from NOAA 12 AVHRR images. Points correspond to individual pixels in the volcanic clouds. *a*, The cloud from the Rabaul eruption, at 09:00 UT on 19 September 1994, shows marked positive band 4 – band 5 temperature differences. *b*, The cloud from the Klyuchevskoi eruption, at 06:30 UT on 1 October 1994, shows negative band 4 – band 5 temperature differences more typical of volcanic clouds. The simulated temperature results (lines in the figure) are compared with actual pixel values (points in the figure) for both eruptions, but for Klyuchevskoi we compare theoretical volcanic ash, based on refractive index data and lognormal size distributions following the method of Wen and Rose¹⁰. For the Rabaul data we follow an analogous approach using refractive-index data for ice and a



lognormal size distribution. For both figures the measured values of optical depth are plotted as dashed near-vertical lines, and effective radius is plotted as arcuate solid lines.

suggest that disturbance of the region around the vent resulted in ready access for sea water to the vent, and that once the sea water came in contact with the magma, it was vaporized and added to the convecting eruption column. Water droplets and ash particles interacted in the lower column, resulting in the evaporative formation of salt crystals¹⁶. The convecting column with its high content of water was cooled as the column rose to 20 km. The ash surfaces in the eruption column continued to nucleate liquid water and ultimately formed ice at temperatures below -40°C (refs 17, 18). The dominance of the ice signal in the AVHRR satellite data is explained by ash being encased within ice in this cloud. The formation of ice in volcanic clouds probably accelerates ash fallout by increasing the diameter of cloud particles³.

We speculate that SO_2 concentrations in the cloud are limited by the accumulation of water droplets, supercooled water and eventually ice around ash nuclei⁴. The mass of SO_2 dissolved in supercooled water (and subsequently trapped in ice) can be estimated at 20–100 kt using the methods of Tabazadeh and Turco⁶ for a volcanic cloud at an altitude of 14 km with a total ice mass of 200–300 Mt (based on the data discussed above). The participation of sea water in the eruption column may thus account for the low amounts of SO_2 detected by TOMS in the case of Rabaul's eruption. We note for example, that in the case of Mount St Helens in 1980 the rates of SO_2 release measured during the climactic eruption were orders of magnitude higher than the rates measured after the eruption, during an open vent condition¹⁹. In contrast, the measurements by TOMS at Rabaul on 29 September (from Tavurvur) were almost the same as those detected during the main Vulcan eruption. In the record of TOMS data since 1979, most stratospheric eruptions, even 'sulphur-poor' ones, have released at least several hundred kilotonnes of SO_2 (ref. 20). These data are consistent with the speculation that much more SO_2 was released during the Rabaul eruption, but that it was scavenged by the H_2O -rich fallout. We speculate that past eruptions with similar sea-level or lake locations (for example, Krakatau²¹, Taupo²² and Santorini²³) could also have been influenced by ice formation, which reduced the length and severity of their influence on the atmosphere by enhancing the removal of both sulphur and ash. We also speculate that the broad 'fan-like' dispersion pattern of the cloud could partly reflect seawater interaction, inducing vorticity by evaporation of water droplets at the cloud edges^{24,25}.

Our results demonstrate the utility of multi-wavelength remote sensing in identifying the constituents of volcanic clouds. Our observations are also relevant to the problem of mitigating the hazard posed to jet aircraft by volcanic clouds that contain silicates which can damage and stop their engines¹. Although they do not display the radiative signal of silicate particles, clouds like Rabaul's may still be hazardous to aircraft, because although ice makes up much of the mass of the cloud, the particles probably have silicate cores. The design of airborne devices to discriminate between water/ice clouds and volcanic ash clouds for aircraft hazard mitigation purposes²⁶ should try to address the eventuality posed by the Rabaul example. We note that there are many Western Pacific and Indonesian volcanoes near important air routes and with settings similar to Rabaul²⁷, and many of these volcanoes have drifting cloud patterns that either disperse in broad fans²⁸ or bifurcate²⁴. □

9. Porter, S. C. in *Tephra Studies* (eds Self, S. & Sparks, R. S. J.) 135–160 (Reidel, London, 1981).
10. Wen, S. & Rose, W. I. *J. geophys. Res.* **99**, 5421–5431 (1994).
11. Prata, A. J. *Geophys. Res. Lett.* **16**, 1293–1296 (1989).
12. Holasek, R. E. & Rose, W. I. *Bull. volcan.* **53**, 420–435 (1991).
13. Schneider, D. J. & Rose, W. I. *Bull. U.S. geol. Surv.* **2047**, 405–418 (1994).
14. Riehle, J. R., Rose, W. I., Schneider, D. J., Casadevall, T. J. & Langford, J. S. *Eos* **75**, 137–138 (1994).
15. Krueger, A. J. et al. *J. geophys. Res.* (submitted).
16. Gilbert, J. S. & Lane, S. J. *Bull. volcan.* **56**, 398–411 (1994).
17. Houze, R. A. *Cloud Dynamics* (Academic, New York, 1993).
18. Hobbs, P. V. & Rangno, A. L. *J. atmos. Sci.* **42**, 2523–2549 (1985).
19. Symonds, R. B., Rose, W. I., Bluth, G. J. S. & Gerlach, T. *Rev. Miner.* **30**, 1–66 (1994).
20. Bluth, G. J. S., Schnetzler, C. C., Krueger, A. J. & Walter, J. S. *Nature* **366**, 327–329 (1993).
21. Sigurdsson, H., Carey, S. N. & Mandeville, C. *Nat. geogr. Res. Explor.* **73**, 310–327 (1988).
22. Walker, G. P. L. *J. Volcan. geotherm. Res.* **8**, 69–94 (1980).
23. Bond, A. & Sparks, R. S. J. *J. geol. Soc. Lond.* **132**, 1–16 (1976).
24. Ernst, G. G. J., Davis, J. P. & Sparks, R. S. J. *Bull. volcan.* **56**, 159–169 (1994).
25. Srivastava, R. C. *J. atmos. Sci.* **44**, 1752–1773 (1987).
26. Barton, I. J. & Prata, A. J. *Bull. U.S. geol. Surv.* **2047**, 313–317 (1994).
27. Johnson, R. W. & Casadevall, T. J. *Bull. U.S. geol. Surv.* **2047**, 191–197 (1994).
28. Sawada, Y. *Tech. Rep. met. Res. Inst. (Jap.)* **22**, 1–335 (1987).

ACKNOWLEDGEMENTS. We acknowledge conversations with T. Gerlach, R. Turco, P. Hobbs and S. Williams, and thank P. Newman for giving us access to radiosonde data, W. Johnson for help with communications and J. Crisp for reading the rough draft and helping to improve it. G.G.J.E. acknowledges R. S. J. Sparks, J. P. Davis, P. Leonard, F. Wheeler, W. Bowery for collaborative support and inspiration, a NERC Assistantship (BRIDGE program) and the 1994 award from the Fondation Belge de la Vocation. W.I.R., D.J.D., D.J.S. and G.J.S.B. were supported by NASA through the Volcano/Climate program.

Received 16 February 1995; accepted 10 May 1995.

1. Casadevall, T. J. *Bull. U.S. geol. Surv.* **2047**, 1–450 (1994).
2. Self, S., Rampino, M. R. & Barbera, J. J. *J. Volcan. geotherm. Res.* **11**, 41–60 (1981).
3. Rose, W. I. & Chesner, C. A. *Geology* **16**, 913–917 (1987).
4. Pinto, J. P., Turco, R. P. & Toon, O. B. *J. geophys. Res.* **94**, 11165–11174 (1989).
5. Bell, D. A. & Saunders, C. P. R. *Atmos. Envir.* **A25**, 801–808 (1991).
6. Tabazadeh, A. & Turco, R. P. *Science* **260**, 1082–1086 (1993).
7. Turco, R. P., Toon, O. B., Whitten, R. C., Hamill, P. & Keese, R. G. *J. geophys. Res.* **88**, 5299–5319 (1983).
8. McKee, C., Johnson, R. W., Lynch, J., Dzurisin, D. & Miller, C. D. *Bull. Glob. Volcan. Network (Smithsonian Inst.)* **19** (9) 4–7 (1994).